

## Molecular Modeling Directed by an Interfacial Test Apparatus for the Evaluation of Protein and Polymer Ingredient Function in Situ

GEORGE W. COLLINS, AVANI PATEL, ALAN DILLEY, AND DIPAK K. SARKER\*

Chemical Biology Research Group, School of Pharmacy and Biomolecular Sciences, The University of Brighton, Moulsecoomb Science Campus, Lewes Road, Brighton BN2 4GJ, United Kingdom

A simplified apparatus is described that measures the damping of a suspended measuring device. The movement of the device (bob) is damped by the properties of the air–water surface adsorbed material. Its value lies in describing the surface chemomechanical properties of ingredients and excipients used in food, nutraceutical, cosmetic (cosmeceutical), and natural drug–food product formulations that traverse the food sciences. Two surfactants, two food and drug-grade polymers, and five naturally occurring food and serum proteins were tested and used to estimate and model interfacial viscoelasticity. Equilibration times of > 15 min were found to give sufficiently stable interfaces for routine assessment. The viscoelasticity of the air–water interface was estimated with reference to model solutions. These model solutions and associated self-assembled interfacial nanostructured adsorbed layers were fabricated using a preliminary screening process with the aid of a specialized foaming apparatus ( $C_{300}$  values), surface tension measurements (23–73 mN/m), and referential surface shear and dilation experiments. The viscoelasticity measured as a percentage of surface damping ( $D$ ) of a pendulum was found to range from 1.0 to 22.4% across the samples tested, and this represented interfacial viscosities in the range of 0–4630  $\mu\text{Ns/m}$ . The technique can distinguish between interfacial compositions and positions itself as an easily accessible valuable addition to tensiometric and analytical biochemistry-based techniques.

**KEYWORDS:** Protein surfactant; damping; viscosity; cross-linking; interface

### INTRODUCTION

Food and industrial formulations make use of mixtures of proteins as product functionalizers, polymers, and chemical processing aids such as surfactants and food emulsifiers or lipidic excipients (8, 18). Foods and products having primary ingredients consisting of native and chemically modified food proteins, polysaccharides, and lipids are widespread (6) and can include simple natural foods themselves, “synthetic foods”, and pharmaceutical dispersions (3, 9). The interplay of ingredients and its effect on the macroscopic behavior of food and therapeutic products remains an area of significant interest because of quality and economic considerations. Shelf life and compositional variations are of interest to food manufacturers and processors alike (19, 28). Investigation of the inclusion of antioxidants and interfacial effects on lipid autoxidation in food based on oils (12) is deemed important to the modeling and prediction of product shelf life. The role of new “purpose-built biosurfactants”, food nutrient status, textural properties, and breakdown compounds such as Maillard reaction products becomes an important feature of mass-produced goods that are

based on coarse or nanodispersions. These can include cereals (dough, cakes, confectionary, etc.), milk protein-based dispersions and gels, edible oils, products for parenteral nutrition or therapy, and nutraceutical–cosmeceutical oils and lotions (8).

The notion of competitive adsorption of surfactants and proteins has been studied over a period of time and is illustrated to good effect in surface dilation and foam film experiments (21). Additionally, competitive displacement and adsorption between a synthetic polymer and lauryl sulfate (SDS) soap have also been studied for the purposes of evaluation of binding capabilities (18), and serum albumin–lipid interactions have been studied for use in microencapsulation (that might be extended to food volatiles and flavor) applications (8).

When applied to investigations concerning dispersed product stability, this has been related to the formation of a water cushion covering the polymer or protein and the molecular freedom of the chains on the surface of a colloidal particle that can permit protein attachment (e.g., serum complement system proteins) in the case of polymer-coated drug particles, such as liposomes (9, 26). This response has been observed for ethylene oxide and propylene oxide block copolymers such as pluronics, poly(ethyleneglycol), and poly(lactide-*co*-glycolide). The interconversion between a flattened “mushroom” and an upright “brush” surface (and various intermediary) forms of surface adsorbed polymer-

\* Author to whom correspondence should be addressed [e-mail d.k.sarker@brighton.ac.uk; telephone +44 (0) 1273 642074; fax +44 (0) 1273 642674].

like material is thought to both influence both drug product stability and have a bearing on the stability of protein-based food foams and emulsions (21–24) via steric repulsion, obstruction of contact, and interaction with the entrained foam lamella liquid. With particulate dispersions, protein or polymer dehydration and removal of this water “cushion” lead to aggregation of the particles (3) and subsequent flocculation, and with foams and emulsions this can increase the extent of “natural” creaming and coalescence (23–25). The movement of small molecules, such as emulsifiers, within the gelled adsorbed layer, considered as aggregates or a network with micro- and nanoscale defects (10), can relate to the behavior of complex systems and is thought to affect gross textural properties.

The interface, in addition to being interesting in its own right, represents an ideal planar (more simplified) model environment for examination of molecular complexing and cross-linking processes and how they influence food quality in addition to chemical instability and incompatibility. The aim of our work has been to produce a simplified surface rheometer to screen interactions that might occur between surface-active biological and synthetic food polymer molecules in an attempt to supplement sometimes inconclusive spectrophotometric and light-scattering methods and complex bulk rheology. Adsorbed protein is often modeled as a continuous gel network, and the exchange of covalent bonds such as disulfide bonds or ester linkages becomes important. Under appropriate conditions this can be modeled by surface rheology so that elements of chemistry, not simply mechanical properties, can be identified (27).

Over the past decade a number of impressive techniques, in terms of the labor investment and study required for their setup, have been used to examine interfacial mechanics. Most of the techniques have the limitations of extensive calibration and investigation for their routine use and the production of complex and customarily unclear data. Among these techniques there are some techniques that have contributed significantly to general understanding.

Ariola et al. (2) used interfacial rheology for shear (tearing) and dilation (stretching; dilatation) of the interface using a Langmuir trough, and this was considered to provide more of physical but not biochemical description; however, this could depend more on the experimental setup. We might look to undertake such experiments in any enzyme-based future work. Techniques such as surface dilation (21, 22) and surface shear rheology have been used for monitoring protein–protein interactions and Maillard condensation products such as lipid–protein and polysaccharide–protein conjugates (28). Rheology using a Du Noüy ring and Langmuir trough with mathematical fitting has been used for comparable output to our method providing “actual” values. The precise magnitude of these values and their interpretation remain a matter of some speculation, and this was obtained after extensive work. The protein and melanoidin–polysaccharide fraction of coffee was assessed by measurement of interfacial elasticity using oscillatory shear with a Du Noüy ring, and this was related to a kinetic model of network formation (19).

Our approach is to use the simplest description that might help us resolve small but significant changes in surface composition and could involve pendant polymer chains that dip into the bulk aqueous phase and are associated with a cushion of protective water. In some cases, this might be resolved (in full or in part) by nanorheological means (1, 6) such as atomic force microscopy (AFM), but this is a technique that is difficult to use and is often seen as an expensive and largely inaccessible technique for routine applications. Food apoproteins and lipid

isolated from egg yolk that play a vital role in the use of egg and its functionality in food were investigated in this manner (6). Both AFM and Langmuir trough works were used to observe structure and relate this to interfacial rheology. Two types of general behavior were observed: aggregates of interfacial material (measured as a viscous system) and extensive network formation that may relate to nanoscale aggregations of material but that clearly exist as a network (measured as a viscoelastic system).

In another approach surface rheology was estimated by a capillary wave method that indicated the major difference between surfactant-based (fluid-like) and polymer- or protein-based (highly viscous or rigid-like) interfacial adsorbed layers (17). In both cases the insoluble Gibbs or Langmuir monolayers were dependent on moiety spreading, diffusion to the interface (controlled by bulk concentration), to form a “tough” interfacial film. The properties of casein films were estimated using the additional experimental methods of ellipsometry and X-ray scattering, and this was used to build a picture of interfacial composition (4). Rheological studies here were based on a float but made use of reflected light and a magnet to drive the oscillations that indicate surface properties and provided a “shear elastic constant”, aimed to unravel the determinants of network formation and link this to coarse dispersion stability. In this case evidence of protein multilayers was seen with  $\beta$ -casein at the air–water interface. Surface rheology has also been assessed using an oscillating bubble method (16), but that took 17 h of equilibration and a pendant drop approach (7). These two techniques represent “real food foams and emulsions” in some sense in that they deal with small curved interfaces. Across many considerations, such as ease of use and simplicity of function, they might be seen as less suitable approaches than our equipment for the mass screening of samples but did yield results of high quality. The techniques were used to provide information on the mechanisms of interfacial mechanics, interfacial competition, structuring, synergism, complexation, and binding, and extrapolation to real systems is not always relevant to model systems.

We aim to provide data to support the routine use of a simplified apparatus that performs the same generalized functions as some of the more theoretically oriented methods described above but that can be applied to solutions (and ultimately oil–water interfaces) to provide a more usable form of information but that builds on work already undertaken to allow a fuller understanding of interfacial amphiphile behavior and its ultimate role in determining the quality of foods.

## MATERIALS AND METHODS

Solutions were prepared using biological and synthetic pharmaceutical polymers and surfactants (low molecular weight detergents and emulsifiers). Protein samples used included bovine serum albumin (BSA; type A2153 fraction V, purity 96%, lot 26H1013; 67 kDa), human serum albumin (HSA; type A9511, purity 97–99%, lot 24H9314; 67 kDa),  $\beta$ -lactoglobulin (BLG; type L0130, purity 90%, lot 033K7003; 18.6 kDa), casein (type C7078, lot 100K0223; 24 kDa), and urease type III isolated from jack beans (UJB; type U1500, lot 88H7000; 545 kDa) all supplied by the Sigma Chemical Co. (St. Louis, MO). Surfactants used included sodium dodecyl sulfate (SDS; type 166-100, purity >99%, batch 16416; 288 Da) and Tween 20 (T20; product 93773; 1.25 kDa) from Fisher (Loughborough, U.K.) and Fluka (Gillingham, U.K.), respectively. Amphiphilic ethylene oxide–propylene oxide copolymer drug delivery pluronics used were F68 NF pastille (Poloxamer 188, Flocor; product G0990395, lot WPYY-647C; 8.4 kDa) and F108 NF prill (Poloxamer 338; product 583062, lot WPMX-543B; 14.6 kDa), obtained as a gift from the BASF Corp. (Mount Olive, NJ). All solutions and cleaning were undertaken with surface chemically

**Table 1.** Estimated Air–Water Surface Tensions for a Range of Surface-Active Proteins, Polymers, and Low Molecular Weight Surfactants at pH 7.0 in 50 mM Phosphate Buffer after Equilibration for 10 min at 20 °C

sample	concentration ( $\mu\text{M}$ )	CMC ( $\mu\text{M}$ )	protein (P), pluronic (X), or surfactant(S)	surface tension <sup>a</sup> (mN/m)
water				73 $\pm$ 1
Tween 20	1	50	S	48 $\pm$ 2 (28)
SDS	1	1000	S	53 $\pm$ 1 (23)
BSA	1		P	58 $\pm$ 1 (52)
BLG	1		P	54 $\pm$ 1 (51)
casein	1		P	58 $\pm$ 2 (50)
F68	1	5	X	52 $\pm$ 2 (40)
F107	1	10	X	53 $\pm$ 2 (40)*

<sup>a</sup> Parentheses following the 10 min equilibrium surface tension data for 1  $\mu\text{M}$  solutions indicate the minimum in the surface tension (mN/m) corresponding to a plateau in the tension versus concentration for each amphiphile. \* Hydroxypropyl cellulose (HPC) and other derivatized celluloses that are polymers in comparison may give surface tensions of 41–48 mN/m (16).

pure water (surface tension = 72.8 mN/m); all active ingredients were prepared in 50 mM phosphate buffer, pH 7.00, unless otherwise specified. All glassware was cleaned routinely with sulfochromic acid. However, materials that might have been corroded by such cleaning, for example, the conductance electrode and the measuring head device, were cleaned by soft abrasion using a dilute Tween 20 solution, followed by copious rinsing with pure water.

A very limited number of surface rheology experiments involving BSA were undertaken at pH 5.6 in 50 mM citric acid–phosphate buffer to mimic the conditions used for calibration with accrued experimental data (refer to **Table 2**). The materials used in the Max-Planck data were BLG (type L0130, lot 91H7005) and BSA (type A7030, lot 11H0107), supplied by the Sigma Chemical Co., and T20 (Surfact-Amps preparation 10%, type 2830), supplied by Pierce (Rockford, IL).

**Foam Stability and Bubble Composition ( $C_{300}$ ).** The technique involving measurement of conductivity was used to probe variations in interfacial composition and to estimate appropriate ratios in binary solution mixtures of polymer and low molecular weight surfactants. The experimental setup is illustrated in **Figure 1**. The configuration is different from previous work, but the principle of operation is well-known and well understood (20–22). Foam stability is defined as the residual conductivity ( $C_{300}$ ) of an intact foam remaining after 300 s of drainage and the sampled stable thin liquid films (TLFs) (5). Previous work has demonstrated that this approach can be used to map interfacial effects (20, 21) and their extrapolation to the bulk stability (liquid retention) in foams. Because the ionic strength of the buffered solvent is high (50 mM), the technique measures the “volume of entrained liquid” between two electrode wires spaced 5 mm apart but positioned within the body of the foam. Foam drainage shows a typical decay curve (**Figure 1**, panel A). The terminal value after 5 min from the foam column reaching a particular height (23) provides an indication of the residual water held within the foam and can be used to compare samples of pure proteins or mixtures of surface-active agents at a fixed molar ratio (*R*).

**Surface Tension.** Samples of 20 mL portions of the liquid tested were allowed to thermally equilibrate for a period of 10 min. A roughened glass microscope slide used for the Wilhelmy plate (2  $\times$  2  $\times$  0.02 cm) method was used to determine the interfacial composition and surface tension (mN/m) using a torsion balance and the appropriate weight of detachment from the air–water interface. Pure water was found to have a value of 72.8 mN/m at 20 °C (21, 22).

**Interfacial Shear Rheology.** The basis of the experimental technique is the damped oscillation of a pendulum after an initial fixed deformation (**Figure 2a**, lever position A to B). The number of swinging pendulum oscillations is related to the viscoelastic properties of the adsorbed surface layer (24) (when other contributions are neglected) situated in the plane of the interface. Ultimately, the pendulum stops to oscillate, and this is directly related to a surface damping effect on the measuring head over and above that of the bulk aqueous phase or surrounding

air. In its simplest format the apparatus consists of a steel torsion wire, a measuring head (bob), a trigger switch, and the sample solution (**Figure 2a**, panel A). The dimensions of the apparatus and spatial alignment are fixed so that there is equal treatment between samples.

Initial calibration of the pendulum was undertaken in air and water, water providing 292% damping of the number of oscillations in air. All sample measurements were blanked against the damping found for a fresh interface formed on a pure sample of water (surface tension = 72.8 mN/m at 20 °C). In our experimental configuration the 69.2 g magnesium–aluminum alloy, 61.8 mm diameter measuring head (and fixings), and 69.5 mm long copper trigger (**Figure 2a**) dimensions and the bob interfacial immersion are fixed and safeguarded against air movement or other interferences by housing in a protective sheath. The trigger is responsible for completing an electrical circuit (**Figure 2b**) indicated by both a red diode output and recorder square-wave signal (**Figure 2b**, panel B). The number of contacts and hence square-wave signal peaks can be counted (or the entire span measured and thus equated to a number) and related to a surface damping when related to those seen with water. The point when the trigger fails to make contact with the trigger plate, even though the measuring head may still be oscillating, corresponds to the end of the experimental data acquisition for every sample solution.

The standard concentration used was 1.0  $\mu\text{M}$  in studies involving proteins; other concentrations tested are indicated at the appropriate point. Measurements are made by placing 35.0 mL of test solution into a cleaned 9.6 cm diameter, 1.0 cm deep glass dish. The sample was left to surface and thermally equilibrate for at least 2 min, but as a matter of routine and standard practice, for 20 min. Measurements follow an initial 15° deformation of the position of the bob sitting on the surface of the test sample. Measurements were usually related to triplicate repeat runs all undertaken on the same sample. For the purposes of relating damping to estimates of surface viscosity (15), previously unpublished data and sample mixtures used for testing of a new apparatus were used in this study. The vertical location of the measuring head is such that there is no effective immersion into the bulk phase, but the contact angle of the meniscus of the solvent with the sidewall of the bob is very small and close to 0°. The vertical “z” and lateral “x–y” positioning of both the sample dish and the trigger contact post (made from brushed copper tubing) were achieved using a mechanical lift.

## RESULTS AND DISCUSSION

The properties of macroscopic interfaces are thought to represent effective models of the interfacial adsorbed layer of foams and emulsions. **Figure 3** (panel A) shows the difference in initial foam drainage form and rates between foams that are stabilized by proteins and surfactant, respectively. Interfacial adsorption and rheology using a pendant drop model (7) have been used to investigate protein–protein interactions that are relevant to food and dispersion form. It is reportedly the “depth” of these interactions that promotes bubble stability (7, 22). With protein-stabilized foams the thin liquid films (TLFs) separating the bubbles are thicker, and consequently entrained liquid and thus microconductivity values ( $\mu\text{S}$ ) at the same moment in time are higher than with simple surfactant such as SDS. Even after 5 min of drainage, there is more water within a BSA-stabilized foam as compared to an SDS-stabilized foam, despite the bubble size being approximately the same (2 mm diameter). This is thought to be related to the pendant chains of polymer/protein that protrude away from the bubble surface (3, 9, 13, 19, 21, 22, 26).

Foams and their foam lamellae are used to assess the concentrations that relate to fragmentation of the interface on TLFs (5, 13) and foam bubbles (21). At very low molar ratios the adsorbed layer immobilized at the interface is thought to effectively fragment, and this has formed the bases of considerable previous study. The mechanism behind the dissolution of protein–protein interaction as in protein-stabilized foams is thought to be the competitive adsorption of surfactant (6, 20, 21).



**Table 2.** Estimated Air–Water Surface Viscosity [Data in Parentheses Represent First the Surface Viscosity at 6 min and Second the Surface Elasticity ( $\mu\text{Pa} \cdot \text{M}$ ), Supplied for Reference Only] at 10 min at 20 °C and Apparent Pseudo-Equilibrium Conditions versus Measured Percentage Damping That Forms the Calibration To Estimate Surface Viscosity<sup>a</sup>

sample	concentration ( $\mu\text{M}$ )	projected (MPI) surface viscosity <sup>b</sup> ( $\mu\text{Ns/m}$ )	% damping (UoB) <sup>c</sup>
$\beta$ -lactoglobulin (BLG)	1.0	3800 (3028, 0.0)	12.54 $\pm$ 0.6
Tween 20 (T20)/BLG molar ratio, $R = 0.09$	BLG fixed at 1.0	3700 (3493, 0.0)	10.03 $\pm$ 0.4
T20/BLG molar ratio, $R = 1000^d$	BLG fixed at 0.1	70 (10.9, 2.7)	1.67 $\pm$ 0.1
T20/BSA, pH 5.6, molar ratio, $R = 0.05$	BSA fixed at 1.0	3480 (3085, 0.0)	15.42 $\pm$ 0.2

<sup>a</sup> The projected data are based on fitting and extrapolation of the form of actual experimental data ( $R^2 = 0.9\text{--}1.0$ ). The bulk protein concentration of solutions tested is 1  $\mu\text{M}$  except where otherwise specified, and solutions were all made in 50 mM sodium phosphate buffer adjusted to pH 7.00 except where otherwise specified, in this case 50 mM citric acid–sodium phosphate buffer was used. <sup>b</sup> MPI refers to the Max Planck Institut; data collected in the past but not presented, see ref 15 for experimental setup. Extrapolated from data taken at 120–240 s showing a standard deviation of approximately 6%. <sup>c</sup> UoB refers to the University of Brighton equipment. <sup>d</sup> Relates to a system that is dominated by the nonionic surfactant (because of the reduced protein concentration and Tween presence in excess) and in some sense can be “taken to represent” the surface on a Tween/low molecular weight only solution, according to previous foam stability work (20–22, 24, 25).

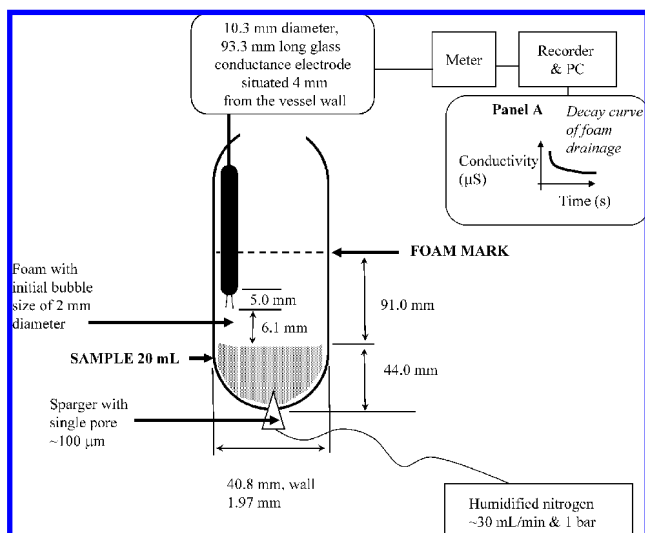


**Figure 1.** Schematic representation of a basic foam stability apparatus used for selection of appropriate mixtures of surfactants and proteins and in some cases polymers (20). Microconductivity gives an estimate of the water entrained in the foam during foam drainage. It can also give an insight into other processes such as bubble rupture and coalescence and indirectly point to interfacial composition. The apparatus in standard format uses 50 mM phosphate buffer at pH 7.0 to over-ride the contributions of the surface active molecules and thereby measure water content. Panel A shows a typical decay curve that is seen with time. The conductivity remaining in the foam after 5 min of drainage is taken to represent a measure of foam stability ( $C_{300}$ ); measurements are undertaken at 20 °C.

This has also been shown to be true for poly(ethylene oxide) polymers and SDS (10).

Panel B within the **Figure 3** shows the familiar foam stability curves for binary mixtures of protein and surfactant (21, 24); the graph can be explained by the alteration in the surface composition following competitive adsorption of surfactant over protein or, in some cases, interfacial replacement. Interfaces that contain less polymer stabilizer tend to give thinner TLFs. As the dissolution of interfacial cross-links between adjacent protein (polymer) molecules is increased within the foam, it becomes more unstable and susceptible to bubble coalescence. This has been studied in detail for food foams and a number of simple model systems (20). The molar ratio ( $R$ ) at which significant dissolution appears is usually considerably less than 1.0. In previous work this has been found to occur at  $R = 0.1$  in dilatational rheology (21),  $R = 0.25$  (22), and  $R = 0.33$  (25), all of which depend on the protein species and its inclination to stay at the interface and the type of surfactant present. In the

protein–surfactant mixtures tested with interfacial rheology here, values of  $R < 0.1$  were used, and these correspond to the initial dissolution of intermolecular cross-links. At very high molar ratios the interface resembles a composition that is similar to that formed from a pure surfactant solution (**Figure 3**, panel B).

Small molecular weight surfactants tend to dominate at the interface when in competition with proteins and polymers. **Table 1** shows the surface tensions of dilute solutions and those at plateau equilibrium concentration (minimum in surface tension). Proteins (BSA, BLG, casein mixtures) generally give surface tensions in the region of 50 mN/m; effective polymeric emulsifiers were found to give equilibrium surface tensions of 40 mN/m, but smaller surfactants are able to significantly reduce the air–water surface tension to  $<30$  mN/m. Given a mixture of BLG and Tween 20, the surfactant or a complex of protein and surfactant (22) has been shown to predominate over the native protein molecule. Previous work has shown that polymers can displace protein from the interface (24), and some studies (16) report on cellulose derivatives having surface tensions of about 45 mN/m. This could be of significance when food gums and proteins are combined in processed foods and a likely subject of future work.

A series of solutions of surface-active molecules were tested for their ability to damp the movements of a probing surface shear device. The results are presented in **Figure 4**; here the effect of equilibration time was demonstrated clearly. In previous theoretical work equilibration times of 12 and 17 h have been considered before equilibrium conditions were achieved. These techniques generally used very large volumes and very dilute solutions (16, 27). One of our primary aims has been to reduce the length of time taken before measurement, and for this reason we do not look to directly measure surface viscosity.

Rheology in various forms can thus be used to test covalent linkages. At present a scientific fixation with absolute measurements (viscoelasticity models;  $G^*$ ,  $G'$ , and  $G''$ ) means the techniques are overly complicated and not used for effective rapid screening of possible formulation candidates as we suggest (27). In the methodologies mentioned by these authors and others, equilibration of the sample took more than half a day for pseudo-equilibrium conditions to be obtained and used up to a quarter of a liter, almost 8 times the volume we use. Because the behavior is very typically “nonlinear”, the surface shear viscosity (stress/strain;  $\eta_s$ ) and its development depend on many variables associated with the experimental data acquisition and the way it is physically sampled; this can ultimately provide difficulties in cross-comparing samples. This is made even more complex when extracted values such as  $G'$  and  $G''$  are extracted from derived mechanical spectra (19).

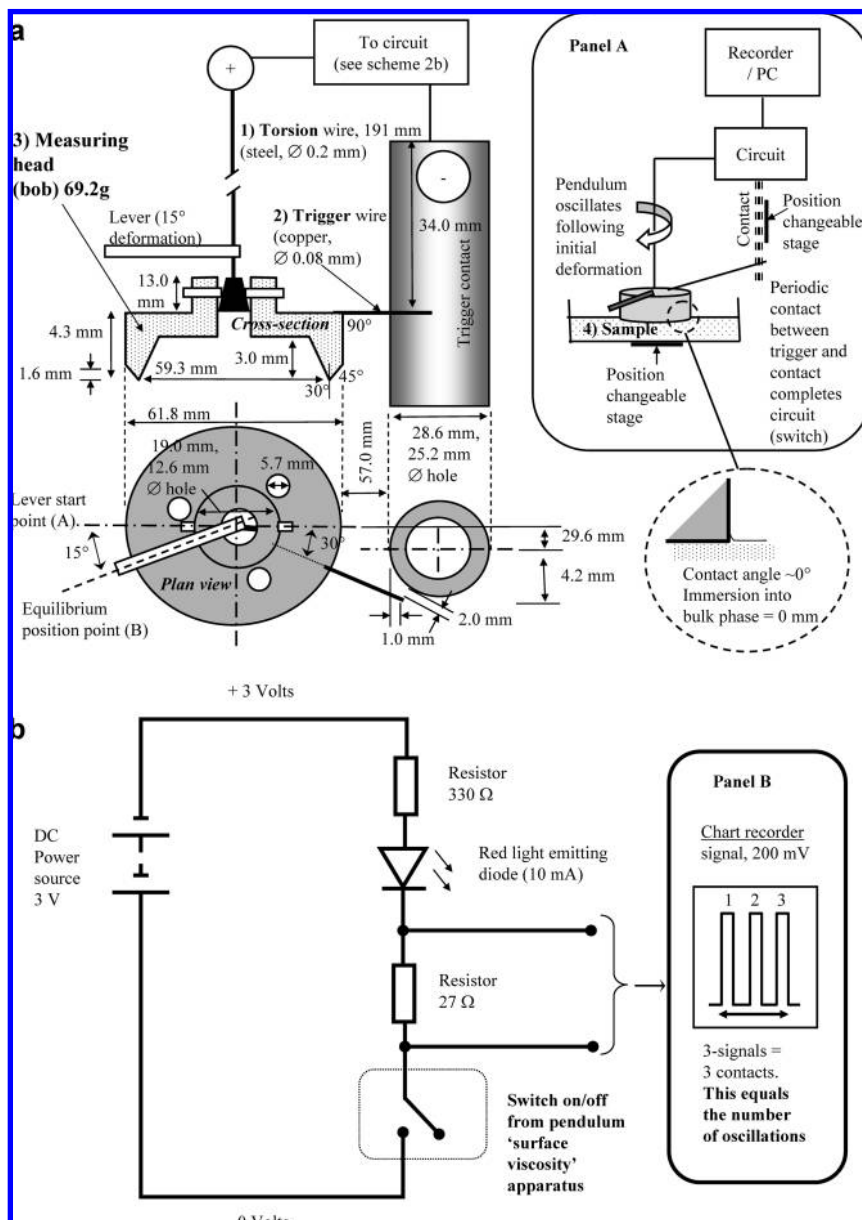


**Figure 2.** Schematic representation of the experimental setup of an air–water surface rheometer. (a) shows the basic components of the instrument: (1) torsion wire, (2) trigger mechanism, (3) measuring head; panel A indicates the fourth major component, which is (4) the sample itself. Within a, panel A shows in the simplest form the basic mechanism of measurement. The pendulum with measuring head fixed on the end has its movement initiated by the lever being released from starting position A to position B. (b) shows a simple representation of the “switch” and acquisition of a square-wave signal based on the number of contacts between the trigger wire and the trigger contact. Damping due to the properties of the interface represents one of a number of contributions to a slowing of the measuring head oscillations. Measurements were undertaken at 20 °C.

According to **Figure 4** low molecular surfactants do not appear to give a significantly more rigid interface when left to surface equilibrate for up to 20 min. With BSA alone and BLG protein in the presence of Tween 20 ( $R = 1000$ ), the percentage damping increased with equilibration time. This in principle corresponds to a stiffening or thickening in consistency of the adsorbed layer, but may also reflect a transition from “elastic” to more “viscous” surface-aggregated (2, 7, 27) adsorbed interfacial material. This was observed in previous studies using bifunctional agents (22, 25) and seen on the aging of the interface that relates to molecular “juggling” and position optimization at the interface (14).

However, with casein and BLG protein in the presence of Tween 20 ( $R = 0.09$ ) the surface damping decreased with equilibration time. In the case of the latter this may be due to

significant rearrangement and dissolution of protein–protein interactions. Recent investigations show that aging (14), with respect to development of significant viscoelasticity, occurs at the interface with proteins. This is explained in terms of the moiety hydrophobicity and the extent of flexibility in the molecule that permit the ease of reformation at the interface, alongside its neighboring molecules that leads to an increase in surface rigidity. This is particularly thought to be the case with many foods for which the textural “elastic form” of material surrounding gas bubbles or fat crystals is an important indicator of quality, such as bread dough and in cakes and pastries.

With casein samples, although the percentage of surface damping decreases between 2 and 90 min, the effect was marginal, and it is difficult to say whether this is a real effect or simply due to experimental variation. Our sample was a

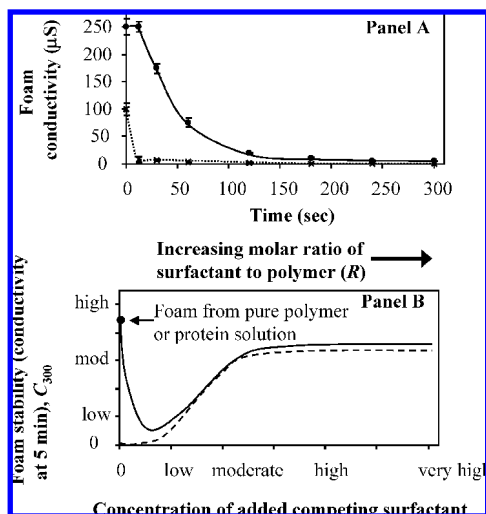


**Figure 3.** Panel A shows foam drainage data for 0.8 mg/mL solution of BSA (12  $\mu\text{M}$ ) pH 7 (●) and 3.5 mM SDS at pH 7 (×) at 20 °C in 50 mM sodium phosphate buffer. Panel B provides an example of typical foam stability curves for low molecular weight surfactant (broken line) a fixed concentration of protein (●) and a fixed concentration of protein/polymer in the presence of increasing low molecular weight surfactant (see refs 21 and 22) indicated by the continuous line. The foaming apparatus can provide information on the point at which a protein-stabilized foam interfacial adsorbed layer begins to be affected by inclusion of a competing surfactant. This was the basis of the mixtures used in rheological studies. The experimental conditions are as indicated above.

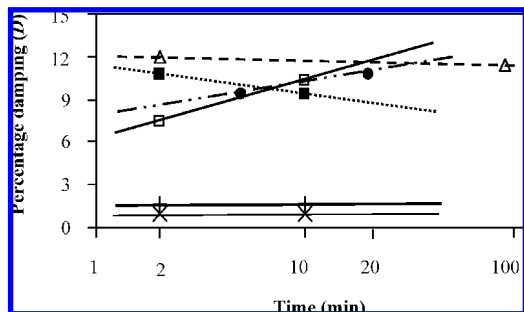


**Figure 4.** Plot showing the changes in surface “stiffness” and percentage damping of a measuring head ( $D$ ) located in the plane of the adsorbed air–water interfacial layer against equilibration time for solutions in 50 mM sodium phosphate buffer at 20 °C. The samples represented are 1  $\mu\text{M}$  BSA (●), Tween 20/BLG mixtures with 1  $\mu\text{M}$  BLG at a ratio,  $R = 0.09$  (■), Tween 20/BLG mixtures with 1  $\mu\text{M}$  BLG at a ratio,  $R = 1000$  (□), 13  $\mu\text{M}$  casein ( $\Delta$ ), 300  $\mu\text{M}$  anionic SDS alone (×), and 100  $\mu\text{M}$  nonionic Tween 20 alone (+). Experimental error in the percentage damping values for each of the samples ( $n = 3$ ) is in the range of 6–7%.

mixture of caseins ( $\alpha_{s1}$ ,  $\beta$ ,  $\kappa$ , etc.), and recent work (4) have shown that the association between  $\alpha_{s1}$  and  $\beta$  (>50% of protein fraction) caseins is primarily responsible for surface viscoelasticity and product functionality in solution or at the interface. In any case, the magnitude of change was negligible, and we suppose that a form of pseudoequilibrium of the interface can be assumed to take place within 20 min given the small volume of sample needed with our apparatus. Given that the equipment’s principal purpose is to compare samples, most measurements were taken after 20 min of thermal equilibration.

The percentage damping that is synonymous with surface consistency increases ( $D$ ) appears as four forms in **Figure 5**. Water and low molecular weight surfactants appear to give

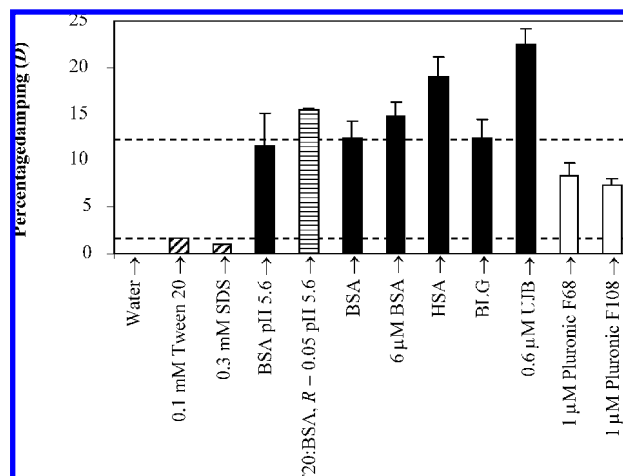


**Figure 5.** Plot showing the percentage damping of a measuring head ( $D$ ) located in the plane of the adsorbed air–water interfacial layer after 20 min of equilibration time for various sample solutions in 50 mM buffer at 20 °C. The samples represented are proteins (black bars), polymer (white bars), mixed protein–Tween (T20) (horizontally shaded blocks), and surfactant (diagonally shaded blocks). Protein concentrations are 1  $\mu\text{M}$ , and the pH of solutions is set at 7.0 except where otherwise stated. BSA samples adjusted to pH 5.6 used 50 mM citric acid–sodium phosphate buffer. The broken lines indicate the values found for BLG representing a strongly viscoelastic surface and that for Tween 20 representing a poorly viscoelastic surface (22). The samples noted as abbreviations are sodium lauryl sulfate (SDS), bovine serum albumin (BSA), human serum albumin (HSA), jack bean urease (UJB), and  $\beta$ -lactoglobulin (BLG). The measurements are based on three or more replicates.

values between 0 and  $\sim 2\%$ , respectively. Interfaces stabilized by protein and a mixture of protein with some incorporated surfactant give much higher values between 12 and 23%, and surface-active polymers (such as poloxamers) give values between 7 and 9%.  $\beta$ -Lactoglobulin that has been studied extensively in terms of dilatational rheology and development of significant surface “elasticity” (21, 22, 25), and constant shear viscometry at the oil–water interface (23) gives a surface damping value of 12.5% and is indicated by the broken line in the figure. Depending on the technique used, this protein is thought to give highly viscoelastic adsorbed layers (21). These are often considered to be in the form of multilayers that are based on a cohesive single primary adsorbed layer of protein molecules (2, 27).

The interplay of food ingredients in a real system such as coffee foam was used to investigate protein–carbohydrate complexes (19). Interfacial effects were considered to be due to the interaction between the lysine amino groups of the protein fraction and carbohydrate ester groups. Other nonspecific molecular interactions in the interfacial layer were thought to be related principally to electrostatic and hydrophobic interactions. The group noted the findings of interfacial measurements, and these correlated well with foam stability as in our case. When the interface is considered to have a significantly high damping value, this correlated well with the  $C_{300}$  values (**Figure 3**) that are higher for BSA than for simple surfactants, such as SDS, that demonstrate weak damping (**Figure 5**), and this is associated with water retention in the TLF subphase in the foam associated with the interfacial presence of hydrophilic polymer (3, 26) as found with colloidal particles.

Two of the proteins examined are distinguished from what might be considered to be conventional model globular proteins

(BLG and BSA) under a range of conditions that have a  $D$  value of 12–15%. In the case of human serum albumin (HSA) this damping is increased by approximately 150% from that measured for BLG, and in the case of jack bean urease (UJB) this value is 180% higher. Both HSA and BSA have the same molecular weight, which is approximately 3.5 times that of BLG, and so it can only be assumed to be related to the extent of interfacial cross-linking that depends on the small-scale molecular differences between BSA and HSA, possibly in the location and number of hydrophobic, charged amino acids, or disulfide bond content (11). In the case of UJB the protein has a molecular weight >29 times that of BLG, and this may explain the scope for greater interfacial cross-linking (2, 14) and entanglement and the subsequent increase in the rigidity and damping of the interfacial layer.

The pluronic samples measured have marginally different molecular weights but seem to contradict this molecular weight related “viscosity” increase. Here, the 14.6 kDa F108 has a lower interfacial viscoelasticity than the F68 species, which is 42% smaller and yet present at the same molar concentration. This could be related to the time of pseudoequilibrium rearrangement, local interfacial conditions (26), diffusion to the interface, and coverage of the surface (3, 9, 10, 18). The smaller species should diffuse more rapidly and may take less time to unfold or reorient at the interface. In either case, it is noteworthy that the  $D$  values for these pluronics (poloxamers) are 40% less than seen with BLG (but ~500% more than with Tween 20). This is obviously related to the diversity of potential cross-links with the BLG overly simple block copolymers such as poloxamers and, thus, margin for development of greater interfacial “viscoelasticity.”

The damping (viscosity, as measured here) is a function of the inertia of the bob suspended as a pendulum and its interaction with both the circuit trigger (via a hair-like spring) and primarily the interfacial adsorbed layer, elasticity in the wire, and a damping provided by both the resistance of the air and viscous drag from the water or other primary solvent used on which the bob rests. The best and most convenient description is explained below as a simplified function with multiple contributions; each of the contributions can have a range of domain values.

$$\text{surface damping parameter } (d) = f(I, E, s, P, W, a) \quad (1)$$

Elemental contributions are indicated as  $I$ , inertia following the 15° initial swing of the pendulum bob;  $E$ , elasticity of the 200  $\mu\text{m}$  diameter, 191 mm long steel wire;  $s$ , elasticity and spring-like damping from the 80  $\mu\text{m}$  diameter copper wire trigger;  $P$ , damping resulting from the surface molecular layer;  $W$ , damping resulting from the interfacial subphase; and  $a$ , damping resulting from the air surrounding the pendulum bob. Major contributions are presented in capital letters, but in our highly standardized model equipment only the damping of the interfacial layer is allowed to vary between experimental runs.

The 69.5 mm copper trigger hair has a  $13 \pm 3\%$  contribution to the normal damping of the pendulum in air ( $150 \pm 2$  full swings); this can be seen as a 5% decrease in the number of swings in a minute when the contact with the trigger contact (Figure 2a) is removed. In any case this is a point of limited further detailed discussion because the equipment was always run with the contact possible for all of our measurements. The contact is needed after all to complete the circuit. What dictates the contact made is the number and extent of swings in the oscillations of the measuring head (bob). These oscillations are directly influenced by interaction between the device measuring

head and molecules located in the plane of the interface. In this manner the technique is superior in many ways to optical-based techniques such as pendant drop or bubble form methods in that a direct physical sampling of the interface takes place and, second, in that the shear rate of the bob is reduced (and thus sensitivity is increased) by this interaction on each marginally less pronounced successive pendulum swing.

The real “apparent” surface viscosity can be estimated with the use of calibration studies. The value of this lies in simply being able to describe events occurring at the surface in another way. These calibration data and experiments were previously performed during collaborative investigations (15). Using a simple fitting program, these can be approximated to our findings with a four-point calibration (see Table 2) to give predicted viscosities ( $\mu\text{Ns/m}$ ) and are described in a minimized form in the following highly simplified relationship ( $R^2 = 0.949$ ,  $n = 4$ ):

$$\text{apparent “predicted” surface viscosity } (\eta_p) = [k_1(\ln D)] - k_2 \quad (2)$$

$k_1$  is a constant of 1719,  $D$  is the percentage damping of the sample, as the surface damping parameter ( $d$ ) compared to that seen with a clean interface from pure water, and  $k_2$  is a constant of 713.

The constants in this case are dimensionless values and simply scale the viscosity against the percentage damping. The first point worth noting is the good fit between extrapolated surface viscosity and damping described above. The apparent viscosities are based on an extrapolated value after 10 min ( $\eta_e$ ) with a correlation coefficient close to 1.0 for each of the values shown in Table 2 and incorporated into the testing regime, based on real experimental data acquired up to 6 min (15). In our case fuller equilibration time is always taken as 20 min (at least 10 min), even though preliminary experiments (Figure 3; Table 2) indicate that the equilibration time, particularly for polymer-stabilized interfaces, takes longer than the 2–6 min to reach plateau pseudo-equilibrium values. The more “retarding” the interaction between the metal bob (measuring head) and the surface the higher is the percentage damping. As can be seen from Figure 4 the damping for a solution of 0.02 mg/mL (1  $\mu\text{M}$ ) BLG is about 12.5% (Table 2), about 10 times greater than that seen with a submolar surfactant solution interface (Figure 5).

In our system we are unable at present to disaggregate the “elastic and viscous” components of the measured damping parameter. However, this might be undertaken as part of future studies, but we do not consider this to be as important as the ability to compare samples for future envisaged evaluation. What is clear from our data is that the elasticity is customarily lower when the viscosity is higher (compare values in parentheses in Table 2, for protein mixtures); very low elasticities are to some extent “inventions”, possibly created by inappropriately “timed” evaluation of Gibbs-type surfactant monolayers or mathematical dissection of raw data. Similarly, the technique described here measures percentage damping, and although it is clear that there is some effect for simple surfactants, the values are surprisingly high when compared to known “viscoelastic” protein-based interfaces such as that formed from BLG or BSA solutions (~14% of the value for BLG alone). This is repeatedly observed for the measured damping for Tween 20 and SDS interfaces, which are essentially “fluid-like” but provide a definite positive  $D$  value (Figure 4) when compared to a fresh interface formed on water. It may also suggest that our technique is able to “see” very low surface viscosities. The other real value of the novel



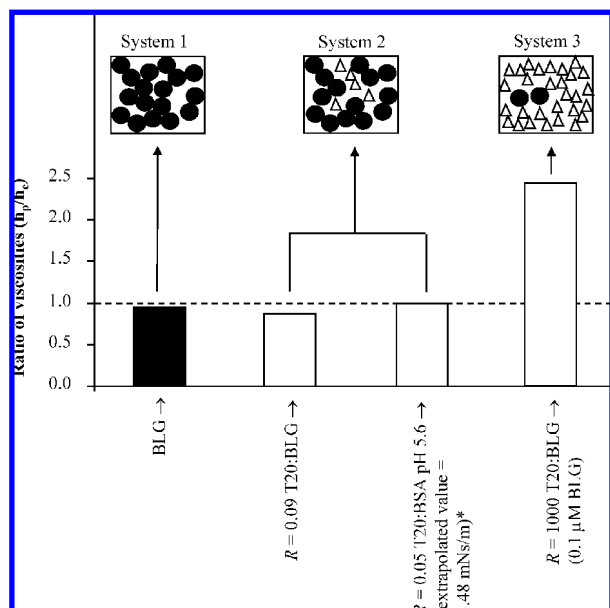


**Figure 6.** Plot showing the ratio-fitted predicted viscosity ( $\eta_p$ ) to actual experimental (projected) viscosity ( $\eta_e$ ) as indicated in **Table 2** and conditions given therein using a measuring bob located in the plane of the adsorbed air–water interfacial layer. The fitted data ( $\eta_p$ ) relate to measurements after 20 min of equilibration time for various sample solutions in 50 mM buffer at 20 °C. The actual data ( $\eta_e$ ) represent extrapolation of the viscoelastic properties of identical solution surfaces from data obtained between 2 and 6 min of equilibration to 10 min. In both cases the geometries of the measuring devices used for surface rheology were similar but not identical. The samples represented are proteins (black bar) and mixtures of protein with Tween (T20) (white bars). Protein concentrations are 1  $\mu$ M, and the pH of solutions is set at 7.0 except where otherwise stated. BSA samples adjusted to pH 5.6 used citric acid–sodium phosphate buffer. The broken line indicates a ratio value of 1.00. An experimentally determined viscosity value for T20/BSA mixtures is indicated (\*) for reference. The plot demonstrates that the predicted and actual extrapolated values are often in very close agreement. The measurements from a fitting procedure represented are based on three or more replicates (experimental variation in values determined is set at approximately 10% in total). The figure also shows a phenomenological interpretation of interfacial composition; three scenarios are considered (referred to as systems 1, 2, and 3). In the model low molecular weight surfactant molecules ( $\Delta$ ) and polymer or protein molecules or nanoscale aggregates of proteins ( $\bullet$ ) that are adsorbed at the interface are shown (not drawn to scale).

apparatus lies in its ability to clearly discriminate and quantify the resistance offered to the metal measuring head. Previous studies have indicated that foam and emulsion thin liquid film form, based on surface adsorbed material is responsible for conferring stability properties on coarse dispersions (19, 21, 22).

Using the estimation it seems that there is a considerably good fitting between the predicted surface viscosity (eq 2,  $\eta_p$ ) and the projection of experimentally monitored viscosities. This can be demonstrated by reference to the ratios presented in **Figure 6**. Here, a ratio of 1.0 indicates that the predicted “surface viscosity” is identical to that of the model data (extrapolated 10 min data) on the basis of results from experiments undertaken at the MPI.

With  $\beta$ -lactoglobulin-stabilized systems the effect of time on spreading of the protein at the interface is of significant interest and extensive contemporary debate. In “pure” protein systems (solutions) this time-related surface equilibrium is considered

to be extensive; however, for mixtures (particularly lipids or surfactants) this equilibrium is generally much shorter, and this can be a consequence of rapid bulk-surface diffusion and the effective competitive adsorption of low molecular weight amphiphiles over polymers. From a range of observations and ancillary measurements (not reported), it appears that globular particles adsorb and then reconfigure slowly over a period of many minutes to hours to form a spreading microheterogeneous mass. This observation is supported by a considerable body of scientific data, including neutron reflectance and atomic force microscopy measurements (6) and many other experimental delineatory approaches. The form of this cross-linked mass is at present not entirely clear, although current thinking points to an aggregate-cross-linked monolayer. There is an equilibrium established between this spreading and the arrival of “new” and the departure of “old” molecules with respect to the interface. Additionally, the way lactoglobulin interacts at the oil/water (O/W) or air/water (A/W) interface is likely to differ significantly from that of nonglobular proteins, such as caseins, or that of the very bulky and rigid globular proteins, such as BSA. The basis of these differences may be related to molecular shape, portion polarity, and molecular rigidity. These differences are likely to affect the surface conformation of the protein and thus its surface damping properties, and also its bulk properties such as viscosity or its ability to form a gel. There is also likely to be “some” difference between the behavior of polymeric amphiphiles at O/W and A/W interfaces, and this has been widely reported over the past two decades.

Four systems were used to compare and in some way give an estimate of a “real” surface viscosity. These were protein alone and three various mixtures of Tween 20 with proteins. The ratio (**Figure 6**) is very close to 1.0 for both BLG and  $R = 0.05$  Tween with BSA systems and slightly less so for the  $R = 0.09$  Tween with BLG system (minus 10%). These ratios were selected because they correspond to the decrease in foam stability on inclusion of competing surfactant discussed at length previously (18, 21, 22, 25). In this way they were considered to be appropriate models for the change from polymer- to mainly surfactant-stabilized interfaces and interesting candidate systems for interfacial modeling.

The fourth piece of data, for diluted BLG and excess Tween 20 ( $R = 1000$ ), does not match as closely to the extrapolated experimental values of 0.070 mNs/m at 0.17 mNs/m and is observed on the plot at a ratio of 2.4. This is still substantially lower than the  $\sim 3.7$  mNs/m viscosity values seen with the proteins tested. It seems that the technique is less substantive for prediction of very low “viscosities” than seen with polymeric systems such as protein-stabilized interfaces. Nevertheless, the technique we use is able to clearly distinguish the properties of a “fluid” (simple surfactant) interface from those of a more rigid (protein) interface, and to this extent the simple and easily applied, rapid technique serves a particular purpose for the examination of foods and pharmaceutical polymer mixtures.

**Figure 6** also shows a cartoon for each of the three distinct types of surfaces thought to exist in the solutions examined. System 1 is an interconnected interfacial layer, showing considerable lateral cohesion, and is thought to exist as a series of interconnected polymer molecules or interconnected aggregates of polymer molecules. This type of system is thought to exhibit considerable levels of viscoelasticity and is envisaged to be present with polymer-only systems or where the level of competing surfactant is too low to have a measurable interfacial impact. System 2 is similar to system 1, but in the former, intermolecular or interaggregate cross-links and connections start



to be lost by positioning of intervening surfactant molecules (13, 19). In this case, an increased interfacial viscosity may be measured at the expense of the “elastic” and rigid nature of the interfacial layer. This was certainly observed for BLG in the presence of lecithin (LPC)-based surfactants using surface dilatational elasticity measurements (21). The third scenario, with an excess of surfactant, resembles the interface in the presence of surfactant alone (with minimal levels of protein inclusion that may or may not have much impact). Here, lateral interactions between adjacent surfactant molecules are weak when compared to those found between proteins, and the interfacial viscoelasticity is low. The second scenario is expected for surfactant–protein molar ratios ( $R$ ) of less than, for example, 0.1 but unlikely to exist at  $R = 1000$ . At such high surfactant concentrations the interfacial layer is fluid and exemplified by our system 3. It is likely that intermediary combinations of all three systems also exist, but this would depend on the protein, its interfacial concentration, and its scope for interfacial desorption and intermolecular cross-linking (4, 14, 27, 28).

An important consideration in the pragmatic use of the results of the rheometer is to assess their value with respect to food and other complex bionanotechnologically related systems (13). In this case, unlike the “model and simplified” systems often described in this paper and the macroscopic planar interfaces examined, there may be interaction between the interfacially adsorbed material and material contained within the bulk phase or entrained liquid that is found within a foam or emulsion lamella. The latter is a common occurrence in protein-stabilized emulsions and foams, particularly with multiphase media such as foods in which there is undoubtedly an interaction between adsorbed layers and polymer, lipid micelles, ice, or other aggregates and crystals (6) that constitute or form part of the dispersion phase. Such interactions are likely to strongly affect damping; however, by using suitable experimental reference environments (solutions) under which this additive behavior is not so pronounced, it may be possible to elaborate further on the mechanisms involved and indicate the extent of such interactions and their relative predominance over the measured effects of the surface adsorbed layer itself. We believe our approach is powerful in that it should enable the user to measure such phenomena, but it will be difficult and challenging to directly disaggregate the individual elements of the measured damping and identify the exact source of this damping directly from the data. Typically, in such a case when the bulk viscosity (consistency; viscoelasticity) and its intrinsic contribution to damping are very high, suitable adjustment may be required or may not be possible. Our aim is to test these possibilities in future work when we progress from simpler systems to more realistic models of “liquid-like” food and pharmaceutical/nutraceutical dispersions.

In experimentally tested (more dilute) solutions, this bulk phase enhancement of measured damping contribution over that of the continuous water phase (taken as a control) is negligible, yet interestingly, it may be possible using suitable time-related calibration studies to get a “scaling” of the depth of this interaction. There is strong experimental evidence to suggest that both thixotropy and rheopexy within the measured surface layer (and subphase) and development of molecular associations and entanglements are time-related events (14). When these types of concentration regimens are used and the likely magnitude of effects seen with highly viscous bulk phases is considered, judgment of this influence over the total measured damping will take a more pragmatic delineatory approach. It is, however, the case that the pendulum device bob and its

vertically tapered “sharp” edge are purposely in contact with the smallest portion of the bulk phase, and thus bulk phase damping tends to minimize given this geometry. At present we have not looked at “solutions or slurries” with this degree of extensive contribution to measured damping, and accordingly at the relevant point some appropriate alterations and a modification to the equipment methodology may be considered.

The foaming apparatus and its ability to predict or reflect interfacial composition is now reasonably well understood (7). Its value lies in providing an additional picture when combined with tensiometry to more fully describe various interfacial structures and their influence on the gross properties of food and other industrial preparations. The composition has an undisputed impact on the physical texture and mouthfeel and visual assessment of shelf life and in some cases on the chemical shelf life of food products by permitting incorporation, sequestration, or exclusion of preservatives (12) or degradation products (19, 28).

There are some drawbacks associated with this new rheological equipment, which include its oversimplification, modular composition, and rapid nature of measurement. For many experienced rheologists this oversimplification presents itself as providing little theoretical information that might be inappropriately judged to reveal little value in the approach. We find the technique more valuable because it generates a numerical index with which to compare samples rather simply than generating elasticity or viscosity values that are obtained from mathematical dissection of an output signal (27). In the case of complex samples this transition between mainly viscous, mainly elastic, and weakly viscoelastic interfaces presents problems in terms of trying to create a simple rationale or replicating experimental conditions for selection of an appropriate mix of ingredients and can be subject to small changes in pH, ionic strength, or temperature, which lead to differing extents of aggregation of polymers with time (14). The technique should be of considerable use to those scientists requiring a simplified picture of the interfacial loading of materials and a reflection of interfacial composition as a route to greater understanding of real food products rather than theoretical work with highly purified food-grade proteins, emulsifiers, and texturizing polysaccharide gums and synthetic polymers. One of our future aims is to test the device on real liquid samples such as beer and milk. The second is to be able to resolve the makeup of solutions following the dissolution of mixtures of powdered ingredients, and the third could involve assessment of the influence of the presence of naturally occurring functionality boosting agents.

In conclusion, the interfacial rheometer is used to assess the damping of adsorbed layers assembled on aqueous solvents. Polymers appear to produce much greater surface damping than simple surfactants. The extension of our work is to use the rheology apparatus to comparatively probe the synergistic or antagonistic effects seen when binary or more complex mixtures of surface-active ingredients are used. Further work might include the actual determination of elastic and viscous elements of the determined surface damping parameter. Although the precise value of this complex information for routine assessment of food mixtures is not clear, the rheometer mentioned here is robust and simple and provides enough detail to be able to test different samples of food ingredients.

#### ACKNOWLEDGMENT

D.K.S. thanks Drs. Jürgen Krägel and Reinhard Miller, formerly at the Max-Planck Institut für Grenzflächenforschung

(MPI), Berlin, for the use (and unpublished data obtained) of a developmental interfacial rheometer.

## LITERATURE CITED

- (1) Al-Hanbali, O.; Rutt, K. J.; Sarker, D. K.; Hunter, A. C.; Moghimi, S. M. Concentration dependent structural ordering of poloxamine 908 on polystyrene nanoparticles and their modulatory role on complement consumption. *J. Nanosci. Nanotechnol.* **2006**, *6*, 3126–3133.
- (2) Ariola, F. S.; Krishnan, A.; Vogler, E. A. Interfacial rheology of blood proteins adsorbed to the aqueous-buffer/air interface. *Biomaterials* **2006**, *27*, 3404–3412.
- (3) Avgoustakis, K.; Beletsi, A.; Panagi, Z.; Klepetsanis, P.; Livianous, E.; Evangelatos, G.; Ithakissios, D.S. Effect of copolymer composition on the physicochemical characteristics, in vivo stability, and biodistribution of PLGA-mPEG nanoparticles. *Int. J. Pharm.* **2003**, *259*, 115–127.
- (4) Beaufils, S.; Hadaoui-Hammoutène, R.; Vié, V.; Miranda, G.; Perez, J.; Terriac, E.; Henry, G.; Delage, M.-M.; Léonil, J.; Martin, P.; Renault, A. Comparative behavior of goat  $\beta$  and  $\alpha_{s1}$  caseins at the air-water interface and in solution. *Food Hydrocolloids* **2007**, *21*, 1303–1330.
- (5) Castelletto, V.; Cantat, I.; Sarker, D.; Bausch, R.; Bonn, D.; Meunier, J. Stability of soap films: hysteresis and nucleation of black films. *Phys. Rev. Lett.* **2003**, *90*, 483021–483024.
- (6) Dauphas, S.; Beaumal, V.; Gunning, P.; Mackie, A.; Wilde, P.; Vié, V.; Riaublanc, A.; Anton, M. Structures and rheological properties of hen egg low density lipoprotein layers spread at the air-water interface at pH 3 and 7. *Colloids Surf. B: Biointerfaces* **2007**, *57*, 124–133.
- (7) David, J. P.; Foegeding, E. A. Comparison of the foaming and interfacial properties of whey protein isolate and egg proteins. *Colloids Surf. B: Biointerfaces* **2007**, *54*, 200–210.
- (8) Dimitrova, M. N.; Matsumura, H.; Dimitrova, A.; Neitchev, V. Z. Interaction of albumins from different species with phospholipid liposomes. Multiple binding sites. *Int. J. Biol. Macromol.* **2000**, *27*, 187–194.
- (9) Dos Santos, N.; Allen, C.; Doppen, A.-M.; Anantha, M.; Cox, K. A. K.; Gallagher, R. C.; Karlsson, G.; Edwards, K.; Kenner, G.; Samuels, L.; Webb, M. S.; Bally, M. B. Influence of poly(ethylene glycol) grafting density and polymer length on liposomes: relating plasma circulation to protein binding. *Biochim. Biophys. Acta* **2007**, *1768*, 1367–1377.
- (10) Erukova, V. Y.; Krylova, O. O.; Antonenko, Y. N.; Melik-Nubarov, N. S. Effect of ethylene oxide and propylene oxide block copolymers on the permeability of bilayer lipid membranes to small molecules including doxorubicin. *Biochim. Biophys. Acta* **2000**, *1468*, 73–86.
- (11) Fleury, F.; Kudelina, I.; Nabiev, I. Interactions of lactone, carboxylate and self-aggregated forms of camptothecin with human and bovine serum albumins. *FEBS Lett.* **1997**, *406*, 151–156.
- (12) Frankel, E. N. Antioxidants in lipid foods and their impact on food quality. *Food Chem.* **1996**, *57*, 51–55.
- (13) Georgiev, G. A.; Sarker, D. K.; Al-Hanbali, O.; Georgiev, G. D.; Lalchev, Z. Effects of poly(ethylene glycol) chains conformational transition on the properties of mixed DMPC/DMPE-PEG thin liquid films and monolayers. *Colloids Surf. B: Biointerfaces* **2007**, *59*, 184–193.
- (14) Hill, K.; Horváth-Szancics, E.; Hajós, G.; Kiss, É. Surface and interfacial properties of water soluble wheat proteins. *Colloids Surf. A: Physicochem. Eng. Aspects* **2007**, . in press.
- (15) Krägel, J.; Wüstneck, R.; Miller, R.; Wilde, P. J.; Sarker, D. K.; Clark, D. C. Assessment of surfactant monolayers at fluid interfaces using a novel pendulum apparatus. *Colloids Surf.* **1995**, *113*, Special Edition: Conference Proceedings of Bubble and Drop 95.
- (16) Mezdour, S.; Cuvelier, G.; Cash, M. J.; Michon, C. Surface rheological properties of hydroxypropyl cellulose at air–water interface. *Food Hydrocolloids* **2007**, *21*, 776–781.
- (17) Monroy, F.; Ortega, F.; Rubio, R. G.; Velande, M. G. Surface rheology equilibrium and dynamic features at interfaces, with emphasis on efficient tools for probing polymer dynamics at interfaces. *Adv. Colloid Interface Sci.* **2007**, *134–135*, 175–189.
- (18) Péron, N.; Mészáros, R.; Varga, I.; Gilányi, T. Competitive adsorption of sodium dodecyl sulphate and polyethylene oxide at the air–water interface. *J. Colloid Interface Sci.* **2007**, *313*, 389–397.
- (19) Pizza, L.; Gigli, J.; Bulbarello, A. Interfacial rheology study of espresso coffee foam structure and properties. *J. Food Eng.* **2008**, *84*, 420–429.
- (20) Sarker, D. K. Sculpted nanoscale polymer films on micrometer bubbles. *Curr. Nanosci.* **2005**, *1*, 157–168.
- (21) Sarker, D. K.; Wilde, P. J.; Clark, D. C. Competitive adsorption of L- $\alpha$ -lysophosphatidylcholine/ $\beta$ -lactoglobulin mixtures at the interfaces of foams and foam lamellae. *Colloids Surf. B: Biointerfaces* **1995**, *3*, 349–356.
- (22) Sarker, D. K.; Wilde, P. J.; Clark, D. C. Control of surfactant-induced destabilization of foams through polyphenol-mediated protein-protein interactions. *J. Agric. Food Chem.* **1995**, *43*, 295–300.
- (23) Sarker, D. K.; Bertrand, D.; Chtioui, Y.; Popineau, Y. Characterisation of foam properties using image analysis. *J. Texture Stud.* **1998**, *29*, 15–42.
- (24) Sarker, D. K.; Axelos, M.; Popineau, Y. Methylcellulose-induced stability changes in protein-based emulsions. *Colloids Surf. B: Biointerfaces* **1999**, *12*, 147–160.
- (25) Sarker, D. K.; Wilde, P. J. Restoration of protein foam stability through electrostatic propylene glycol alginate-mediated protein–protein interactions. *Colloids Surf. B: Biointerfaces* **1999**, *15*, 203–213.
- (26) Vonarbourg, A.; Passirani, C.; Saulnier, P.; Benoit, J.-P. Parameters influencing the stealthiness of colloidal drug delivery systems. *Biomaterials* **2006**, *27*, 4356–4373.
- (27) Wierenga, P. A.; Kosters, H.; Egmond, M. R.; Voragen, A. G. J.; de Jongh, H. H. J. Importance of physical vs. chemical interactions in surface rheology. *Adv. Colloid Interface Sci.* **2006**, *119*, 131–139.
- (28) Wooster, T. J.; Augustin, M. A. Rheology of whey protein–dextran conjugate films at the air/water interface. *Food Hydrocolloids* **2007**, *21*, 1072–1080.

---

Received for review January 14, 2008. Revised manuscript received March 11, 2008. Accepted March 12, 2008.

JF800122K